Colourimetric Determination of High-Density Lipoprotein HDL Cholesterol using Red-Green-Blue Digital Colour Imaging

Camilo L. M. Morais,[1]* Kássio M. G. Lima[2] and Francis L. Martin[1]

[1]School of Pharmacy and Biomedical Sciences, University of Central Lancashire, Preston PR1 2HE, United Kingdom

[2]Biological Chemistry and Chemometrics, Institute of Chemistry, Federal University of Rio Grande do Norte, Natal 59072-970, Brazil

***Corresponding author:** Camilo L. M. Morais, Maudland Building room MB030, School of Pharmacy and Biomedical Sciences, University of Central Lancashire, Preston PR1 2HE, United Kingdom. Tel.: +44 07476 704524. Email: cdlmedeiros-de-morai@uclan.ac.uk

Abstract: A rapid, low-cost and sensitive method for quantification of high-density lipoprotein (HDL) cholesterol based on enzymatic colorimetric reactions and digital image analysis was developed. The proposed method was adapted to a 96-microwell enzyme-linked immunosorbent assay (ELISA) plate and imaging acquisition was performed using a conventional desktop scanner. The images were recorded using the red-green-blue (RGB) colour system in which the resolved absorbance for each colour channel was used for multiple linear regression. The regression model presented a root mean squared error of calibration and R^2 value of 1.53 mg dL^{-1} and 0.995, respectively. Prediction was obtained with a root mean square error of prediction of 2.42 mg dL^{-1} and R^2 of 0.993; therefore, showing a good prediction response. A limit of detection of 0.43 mg dL^{-1} and precision better than 1.72% reinforced these results. This method was compared with a reference methodology using UV-Vis measurements at 500 nm and no statistical difference was observed at a confidence level of 95%; showing its potential for future clinical applications.

Keywords: High-density lipoprotein (HDL) cholesterol; multiple linear regression; enzyme-linked immunosorbent assay (ELISA); colorimetry; red-green-blue (RGB) colour.

Introduction

High-density lipoprotein (HDL) cholesterol is a type of lipoprotein present in serum that plays an important atheroprotective role by modifying cholesterol transport (Nicod et al. 2015). It is normally associated with low-density lipoprotein (LDL) and very low-density lipoprotein (VLDL) cholesterol (Brunham and Hayden 2015). The concentration of HDL cholesterol is an important biomarker towards evaluating health conditions, since low levels of this biomarker in blood serum can be an indicator of cardiovascular diseases (Nicod et al. 2015; Brunham and Hayden 2015; Nakamura et al. 2015). In routine analysis, HDL cholesterol is measured in conjunction with triglycerides, LDL and total cholesterol in monitoring the individual risk of a patient developing cardiovascular diseases (Nakamura et al. 2015).

The measurement of HDL cholesterol is commonly performed using enzymatic colorimetric methods, which is the gold standard for analysing this type of lipid (Menezes 2015). The measurement is typically made employing ultraviolet-visible spectroscopy with a single wavelength response at 500 nm, since the product of the enzymatic colorimetric reaction is quinoneimine, a compound that absorbs at 500-506 nm (Menezes 2015).

Digital image analysis has been widely applied to quantify compounds in the visible range in recent years. It has been employed in applications for food monitoring (Benedetti et al. 2015; Santos and Pereira-Filho 2013; Lyra et al. 2014), environmental assays (Andrade et al. 2013; Firdaus 2014), forensic investigations (Choodum and Daeid 2011; Choodum et al. 2013; Tosato et al. 2016) and clinical analysis (Morais and Lima 2015; Morais et al. 2016; Xia et al. 2015). Digital image processing is commonly employed using the red-green-blue (RGB) colour system. Hereupon, a single image can be translated into millions of colours using a combination of three wavelength responses: red (700.0 nm), green (546.1 nm) and blue (435.8 nm) (Petrou and Petrou

2010). The colour formed can be transformed into many types of analytical signals, such as intensity (Moraes et al. 2014), histograms (Morais and Lima 2015; Diniz et al. 2012) or RGB-resolved absorbances (Christodouleas et al. 2015). The latter makes use of Beer-Lambert law in order to transform the colour intensity of an image into an absorbance-like value where a reference image is used as the blank. Due to the wide range of possible combinations between RGB colour values, commonly multivariate calibration methods are used with image processing. Chemometric methods such as multiple linear regression and partial least squares regressions have been used in many image processing applications (Lyra et al. 2014; Morais and Lima 2015; Morais et al. 2016).

The increasing usage of digital images for analytical applications is a result of the rapid growth of image-acquisition technologies which makes use of cell phones, webcams and scanners, which are very economical and practical (Apyari et al. 2017). In addition to this, the high analytical frequency obtained through fast computational processing and extendable technology for point-of-care applications are some features that make the potential use of digital imaging very attractive nowadays. Herein, we describe a fast, low-cost and sensitive method using a convectional desktop scanner to determinate HDL cholesterol concentrations based on RGB image analysis.

Materials and Methods

Samples

The enzymatic colorimetric reaction for determination of HDL cholesterol was performed using commercial kits. The kits were acquired from Labtest® (Labtest Diagnóstica SA, Brazil)

with reference codes ref. 13 and ref. 76 for HDL cholesterol separation and enzymatic colorimetric reaction, respectively. These kits are traceable to Standard Reference Material 911 from the National Institute of Standards and Technology.

The colorimetric reaction following the reference method took place by reacting 0.1 mL of cholesterol sample with 1.0 mL of a precipitating solution composed of phosphotungstic acid (1.5 mmol L^{-1}) and magnesium chloride (54 mmol L^{-1}). After centrifugation for 15 min at 3500 rpm, LDL and VLD cholesterol were precipitated and HDL cholesterol was collected from the supernatant. Then, 0.01 mL of the HDL cholesterol reacted with 1.0 mL of a buffer mixture (pH 7.0) containing phenol (24 mmol L^{-1}), sodium cholate (500 µmol L^{-1}), sodium azide (15 mmol L^{-1}), 4-aminoantipyrine (500 µmol L^{-1}), cholesterol esterase (≥250 U L^{-1}), cholesterol oxidase (≥250 U L^{-1}) and peroxidase (≥1000 U L^{-1}) for 10 min at 37°C. The reaction is depicted in Figure 1 (Menezes et al. 2015). As a result, a dye called antipyrilquinoneimine is formed proportional to the HDL cholesterol concentration.

[Insert Figure 1 here]

The concentration range studied varied from 0.31 to 52 mg dL^{-1} of HDL cholesterol. In total, 20 samples were measured. Reference measurements were performed using a clinical UV-Vis spectrophotometer BIO-2000 (Bioplus Ltda, Brazil) with absorbance readings at 500 nm. The reference values of HDL cholesterol were obtained after previous instrument calibration.

Image acquisition

Image acquisition was performed using a conventional HP Scanjet G2410 desktop scanner (Hewllet-Packard, USA). For this, 250 µL of the reaction product containing antipyrilquinoneimine was transferred into the microwells of a 96-microwell enzyme-linked

immunosorbent assay (ELISA) plate (Fischer Scientific, USA). In addition, blank samples composed of deionized water were added in the same volumes. The images were recorded with the scanner lid closed in order to avoid interference by external light. Figure 2 depicts an example of a recorded image.

[Insert Figure 2 here]

The images were saved onto a personal computer in .TIFF format with a resolution of 72 × 72 dpi (default scanner settings). Then, the scanned images were loaded into MATLAB® R2014b software (MathWorks, Inc., USA) and the region of interest composed by a squared region with a size of 21 × 21 pixels for each microwell were automatically cropped using a lab-made algorithm.

Computation analysis

Initially, the resolved absorbance values of the R, G and B colour channels for each sample image were calculated within MATLAB® environment. The RGB-resolved absorbance values were used with the Kennard-Stone algorithm (Kennard and Stone 1969) in order to separate the calibration (n=14) and prediction (n=6) sets. The Kennard-Stone algorithm works based on a Euclidian distance calculation assigning the samples more distant to the samples' mean to the calibration set, and the samples closest to the samples' mean to the prediction set. This ensure that the calibration model will cover all sources of variation within the dataset. The resolved absorbance A_k is calculated for each colour channel k as (Christodouleas et al. 2015):

$$A_k = -\log \frac{I_k}{I_{k,0}} \quad (1)$$

where I_k is the colour intensity of channel k (R, G or B) defined as the average value of all pixels in the colour channel; and, $I_{k,0}$ is the colour intensity of channel k of the blank image.

The resolved-absorbance values for each image were concatenated in an array in order to create a matrix $\mathbf{X}$ {n x 3} with n rows (samples) and 3 columns (RGB-resolved absorbances). The $\mathbf{X}$ matrix was used for calibration using multiple linear regression, according to equations 2-4 (Morais et al. 2016):

$$\mathbf{y}_{cal} = \mathbf{X}_{cal}\mathbf{b} \quad (2)$$

$$\hat{\mathbf{b}} = \left(\mathbf{X}_{cal}{}^{\mathrm{T}}\mathbf{X}_{cal}\right)^{-1}\mathbf{X}_{cal}{}^{\mathrm{T}}\mathbf{y}_{cal} \quad (3)$$

$$\hat{\mathbf{y}}_{pred} = \mathbf{X}_{pred}\hat{\mathbf{b}} \quad (4)$$

where $\mathbf{X}_{cal}$ is a matrix containing the RGB-resolved absorbances for the calibration samples; $\mathbf{X}_{pred}$ is a matrix containing the RGB-resolved absorbances for the prediction samples; $\mathbf{b}$ is a vector of regression coefficients; $\mathbf{y}_{cal}$ is a vector containing the concentration values for each calibration sample; $\hat{\mathbf{y}}_{pred}$ is the response vector obtained by multiple linear regression that contains the estimated concentration of the prediction samples; and T represents the transpose matrix operation.

The results were evaluated according to certain figures of merits, including root mean square error of calibration, root mean square error of prediction, relative error in %, relative standard deviation, limit of detection and limit of quantification. The limit of detection and limit of quantification were calculated as follows:

$$\text{Limit of detection} = 3.3\delta_x\|\mathbf{b}\| \quad (5)$$

$$\text{Limit of quantification} = 10\delta_x\|\mathbf{b}\| \quad (6)$$

where δ_x is the standard-deviation of the blank, and $\|\mathbf{b}\|$ is the norm of the regression coefficients **b**.

Results and Discussion

The concentration of HDL cholesterol was obtained by using an enzymatic colorimetric method associated with imaging analysis. Poor linearity on single RGB channels was observed using univariate calibration. For example, the root mean square error of calibration and relative error in % for the calibration set using the colour channel with best linearity (resolved absorbance of B channel, R^2 = 0.912) were equal to 5.41 mg dL^{-1} and 16.22%, respectively. For the prediction set, the root mean square error of prediction and relative error in % were equal to 6.70 mg dL^{-1} and 22.34%, respectively. The relatively low resolution of the images (72 × 72 dpi) can lead to an increasing of the root mean square error of calibration and relative error in % due to the lower level of details in the image. However, the lower image resolution speeds up data acquisition, decreases the storage capacity and improves the computational processing time, therefore being more suitable for routine applications. In order to overcome the limitations of univariate analysis, multivariate calibration was required to improve the prediction model.

Multiple linear regression was applied using the three RGB-resolved absorbances for each sample image. Regression coefficients equal to -429.66, 433.69 and -119.79 were obtained for the R, G and B channels, respectively. Using the multiple linear regression model, the root mean square error of calibration value dropped to 1.53 mg dL^{-1} and the relative error in % in the calibration set dropped to 4.71%. For prediction, the root mean square error of prediction and relative error in % were equal to 2.42 mg dL^{-1} and 8.06%, respectively. Cross-validation leave-

one-out was performed with a root mean square error of cross-validation of 2.43 mg dL^{-1} and R^2 of 0.985. Figure 3 shows the measured versus predicted concentration of HDL cholesterol calculated by multiple linear regression; and additional results for the multiple linear regression model are shown in Table 1.

[Insert Figure 3 here]

[Insert Table 1 here]

The model seems to be linear above 2 mg dL^{-1} (Figure 3), where the predicted concentrations are very close to the measured ones. Below 2 mg dL^{-1}, the sample images and blank appear to have similar colouring and the model is unstable. The limit of detection and limit of quantification for the reference and imaging method are shown in Table 2.

[Insert Table 2 here]

The limit of detection and limit of quantification values of the imaging method were inferior to the reference method due to the sensitivity of ultraviolet-visible spectroscopy over the image sensor, since at low concentrations the reduced image resolution makes it difficult to differentiate the sample from the blank information. However, the higher limit of quantification for the imaging method is not a problem for clinical applications, since the critical level of HDL cholesterol in serum is around 40 mg dL^{-1}. In addition, other figures of merit show good agreement between both techniques, where the precision (relative standard deviation = 1.72%) and recovery (87.10-99.15%) of the image method were close to the reference measurements (relative standard deviation = 1.50%, recovery between 95.00-100%); and no statistical difference was observed at a confidence level of 95% between the results found by the image and the reference method based on a paired *t*-test.

These results are very promising from a clinical point of view, due to its high reliability and low error. For example, the National Cholesterol Education Program indicates a maximum error in HDL cholesterol analysis of 12.8% (Expert Panel on Detection, Evaluation, and Treatment of High Blood Cholesterol in Adults 2001), whereas using image analysis we found 8.06%. Moreover, the imaging method shows advantages over traditional spectroscopy, since it has a higher analytical frequency due to the analysis of an entire ELISA microplate with 96 micro-wells in a single reading; and very low cost, because of the low instrumental cost of the microplate (US$ 4) and scanner (US$ 200) compared to an ultraviolet-visible spectrometer.

Conclusions

This paper reports an imaging analysis method that can be a potential substitute for HDL cholesterol determination. The method was based on a colorimetric enzymatic reaction and adapted to 96-microwell ELISA plate. Images were acquired using a conventional desktop scanner and the data was processed using multiple linear regression. The results were in good agreement with the ones obtained through gold reference analysis, in which no statistical difference was observed at a 95% confidence level. In addition, a low relative error (8.06%) indicates that this methodology may have the potential for clinical applications. The imaging approach has as an advantage a high analytical frequency; low-cost; and, it is open to the possibility of point-of-care tests or applications in remote zones where the infrastructure for clinical analysis is reduced.

Acknowledgements

Camilo L. M. Morais would like to thank CAPES-Brazil (Doutorado Pleno no Exterior, grant 88881.128982/2016-01) for financial support. Kássio M. G. Lima thanks the CNPq grant (305962/2014-0) for financial support.

References

Andrade, S. I. E., M. B. Lima, I. S. Barreto, W. S. Lyra, L. F. Almeida, M. C. U. Araújo, and E. C. Silva. 2013. A digital image-based flow-batch analyzer for determining Al(III) and Cr(VI) in water. *Microchemical Journal* 109:106–111. doi: 10.1016/j.microc.2012.03.029.

Apyari, V. V., M. V. Gorbunova, A. I. Isachenko, S. G. Dmitrienko, and Yu. A. Zolotov. 2017. Use of household color-recording devices in quantitative chemical analysis. *Journal of Analytical Chemistry* 72 (11):1127–1137. doi: 10.1134/S106193481711003X.

Benedetti, L. P. S., V. B. Santos, T. A. Silva, E. Benedetti Filho, V. L. Martins, and O. Fatibello-Filho. 2015. A digital image-based method employing a spot-test for quantification of ethanol in drinks. *Analytical Methods* 7:4138–4144. doi: 10.1039/C5AY00529A.

Brunham, L. R., and M. R. Hayden. 2015. Human genetics of HDL: Insight into particle metabolism and function. *Progress in Lipid Research* 58:14–25. doi: 10.1016/j.plipres.2015.01.001.

Christodouleas, D. C., A. Nemiroski, A. A. Kumar, and G. M. Whitesides. 2015. Broadly Available Imaging Devices Enable High-Quality Low-Cost Photometry. *Analytical Chemistry* 87 (18):9170–9178. doi: 10.1021/acs.analchem.5b01612.

Choodum, A., and N. N. Daeid. 2011. Rapid and semi-quantitative presumptive tests for opiate drugs. *Talanta* 86:284–292. doi: 10.1016/j.talanta.2011.09.015.

Choodum, A., P. Kanatharana, W. Wongniramaikul, and N. N. Daeid. 2013. Using the iPhone as a device for a rapid quantitative analysis of trinitrotoluene in soil. *Talanta* 115:143–149. doi: 10.1016/j.talanta.2013.04.037.

Diniz, P. H. G. D., H. V. Dantas, K. D. T. Melo, M. F. Barbosa, D. P. Harding, E. C. L. Nascimento, M. F. Pistonesi, B. S. F. Band, and M. C. U. Araújo. 2012. Using a simple digital camera and SPA-LDA modeling to screen teas. *Analytical Methods* 4:2648–2652. doi: 10.1039/C2AY25481F.

Expert Panel on Detection, Evaluation, and Treatment of High Blood Cholesterol in Adults. 2001. Executive Summary of the Third Report of the National Cholesterol Education Program (NCEP) Expert Panel on Detection, Evaluation, and Treatment of High Blood Cholesterol in Adults (Adult Treatment Panel III). *Journal of the American Medical Association* 285 (19):2486–2497. doi: 10.1001/jama.285.19.2486.

Firdaus, M. L., W. Alwi, F. Trinoveldi, I. Rahayu, L. Rahmidar, and K. Warsito. 2014. Determination of Chromium and Iron Using Digital Image-based Colorimetry. *Procedia Environmental Sciences* 20:298–304. doi: 10.1016/j.proenv.2014.03.037.

Kennard, R. W., and L. A. Stone. 1969. Computer Aided Design of Experiments. *Technometrics* 11 (1):137–148. doi: 10.1080/00401706.1969.10490666.

Lyra, W. S., L. F. Almeida, F. A. S. Cunha, P. H. G. D. Diniz, V. L. Martins, and M. C. U. Araujo. 2014. Determination of sodium and calcium in powder milk using digital image-based flame emission spectrometry. *Analytical Methods* 6:1044–1050. doi: 10.1039/C3AY41005F.

Menezes, F. G., A. C. O. Neves, D. F. de Lima, S. D. Lourenço, L. C. da Silva, and K. M. G. de Lima. 2015. Bioorganic concepts involved in the determination of glucose, cholesterol and triglycerides in plasma using the enzymatic colorimetric method. *Química Nova* 38 (4):588–594. doi: 10.5935/0100-4042.20150040.

Moraes, E. P., N. S. A. Silva, C. L. M. Morais, L. S. Neves, and K. M. G. 2014. Lima. Low-Cost Method for Quantifying Sodium in Coconut Water and Seawater for the Undergraduate Analytical Chemistry Laboratory: Flame Test, a Mobile Phone Camera, and Image Processing. *Journal of Chemical Education* 91 (11):1958–1960. doi: 10.1021/ed400797k.

Morais, C. L. M., A. C. O. Neves, F. G. Menezes, K. M. G. Lima. 2016. Determination of serum protein content using cell phone image analysis. *Analytical Methods* 8:6458–6462. doi: 10.1039/C6AY01783E.

Morais, C. L. M., and K. M. G. Lima. 2015. Determination and analytical validation of creatinine content in serum using image analysis by multivariate transfer calibration procedures. *Analytical Methods* 7:6904–6910. doi: 10.1039/C5AY01369K.

Nakamura, M., S. Yokoyama, Y. Kayamori, H. Iso, A. Kitamura, T. Okamura, M. Kiyama, H. Noda, K. Nishimura, M. Nakai, et al. 2015. HDL cholesterol performance using an ultracentrifugation reference measurement procedure and the designated comparison method. *Clinica Chimica Acta* 439:185–190. doi: 10.1016/j.cca.2014.10.039.

Nicod, N., R. S. Parker, E. Giordano, V. Maestro, A. Davalos, and F. Visioli. 2015. Isomer-specific effects of conjugated linoleic acid on HDL functionality associated with reverse cholesterol transport. *The Journal of Nutritional Biochemistry* 26 (2):165–172. doi: 10.1016/j.jnutbio.2014.10.002.

Petrou, M., and C. Petrou. 2010. *Image Processing: The Fundamentals*, 2nd edn. West Sussex: Wiley.

Santos, P. M., and E. R. Pereira-Filho. 2013. Digital image analysis – an alternative tool for monitoring milk authenticity. *Analytical Methods* 5:3669–3674. doi: 10.1039/C3AY40561C.

Tosato, F., T. R. Rosa, C. L. M. Morais, A. O. Maldaner, R. S. Ortiz, P. R. Filgueiras, K. M. G. Lima, and W. Romão. 2016. Direct quantitative analysis of cocaine by thin layer chromatography plus a mobile phone and multivariate calibration: a cost-effective and rapid method. *Analytical Methods* 8:7632–7637.

Xia, M., Z. Wang, Z. Yang, and H. Chen. 2015. A novel digital color analysis method for rapid glucose detection. *Analytical Methods* 7:6654–6663. doi: 10.1039/C5AY01233C.

Captions for Figures

Figure 1: Enzymatic colorimetric reaction to determine HDL cholesterol.

Figure 2: Example of ELISA plate containing HDL cholesterol samples.

Figure 3: Measured concentration of HDL cholesterol using ultraviolet-visible spectroscopy with enzymatic colorimetric reactions (absorbance at 500 nm) *versus* predicted concentration of HDL cholesterol calculated using multiple linear regression with the RGB-resolved absorbances of colorimetric images.

Table 1: Results for imaging method using multiple linear regression.

Parameters	**Value**
Calibration	
Worked range (mg dL^{-1})	0.31 – 52.00
Root mean squared error of calibration (mg dL^{-1})	1.53
Bias (mg dL^{-1})	0.56
Relative error (%)	4.71
R^2	0.995
Prediction	
Root mean squared error of prediction (mg dL^{-1})	2.42
Bias (mg dL^{-1})	-0.56
Relative error (%)	8.06
R^2	0.993

Table 2: Relative standard deviation, recovery, limit of detection and limit of quantification obtained for the reference method using ultraviolet-visible spectroscopy and the image method.

Method	**Relative standard deviation (%)**	**Recovery (%)**	**Limit of detection (mg dL^{-1})**	**Limit of quantification (mg dL^{-1})**
Reference using ultraviolet-visible spectroscopy	1.50	95.00 – 100	0.12	0.40
Imaging	1.72	87.10 – 99.15	0.43	1.45

Figure 1

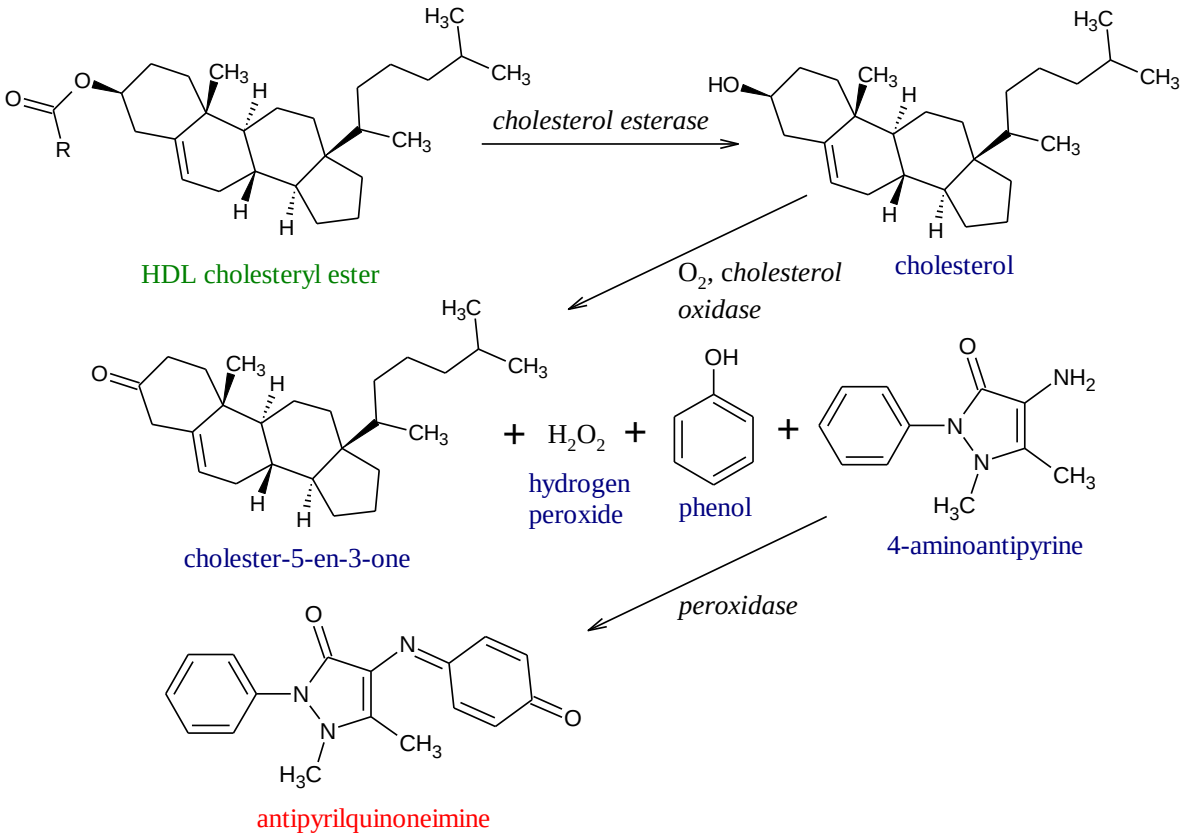
cholesterol esterase
HDL cholesteryl ester
cholesterol
O2, cholesterol oxidase
cholester-5-en-3-one
hydrogen peroxide
phenol
4-aminoantipyrine
peroxidase
antipyrilquinoneimine

Figure 2

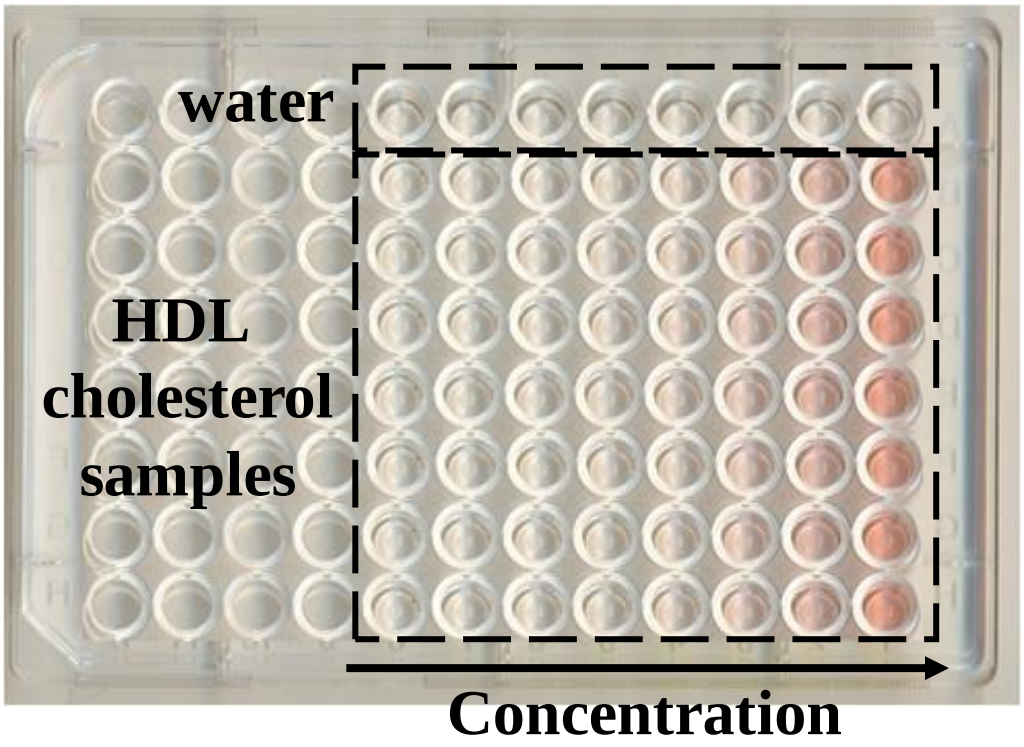

Figure 3

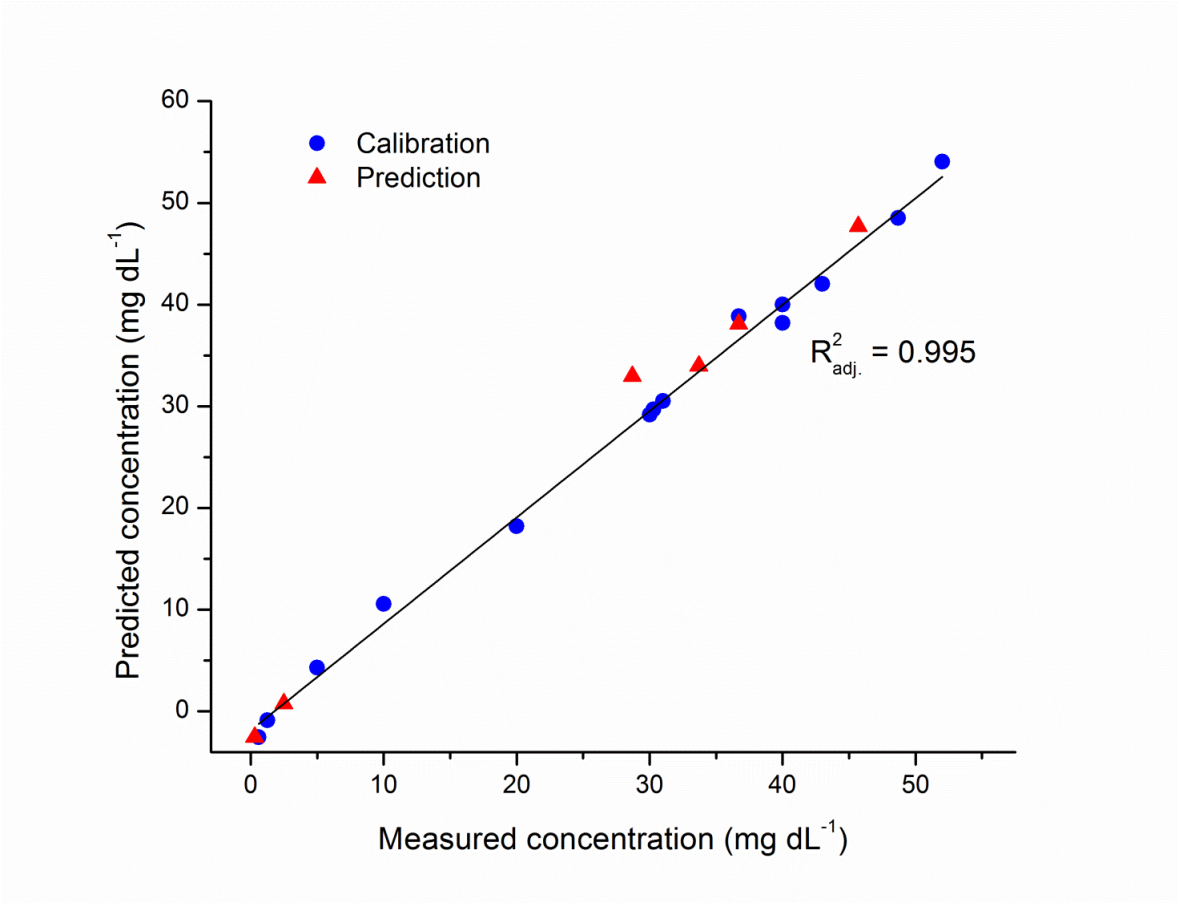
Calibration
Prediction
$R^2_{adj.}$ = 0.995
Predicted concentration (mg dL^{-1})
Measured concentration (mg dL^{-1})
0
10
20
30
40
50
60

Graphical Abstract